



# Diminished band discontinuity at the p/i interface of narrow-gap a-SiGe:H solar cell by hydrogenated amorphous silicon oxide buffer layer

Duy Phong Pham <sup>a</sup>, Sangho Kim <sup>b</sup>, Anh Huy Tuan Le <sup>a</sup>, Jinjoo Park <sup>a, \*\*</sup>, Junsin Yi <sup>a, \*</sup>

<sup>a</sup> College of Information and Communication Engineering, Sungkyunkwan University, Suwon, 440-746, Republic of Korea

<sup>b</sup> Department of Energy Science, Sungkyunkwan University, Suwon, 440-746, Republic of Korea



## ARTICLE INFO

### Article history:

Received 13 March 2018

Received in revised form

17 May 2018

Accepted 21 May 2018

Available online 22 May 2018

### Keywords:

Narrow-gap a-SiGe:H solar cells

a-SiO<sub>x</sub>:H buffer layers

Band gap profiling

## ABSTRACT

We optimized hydrogenated amorphous silicon oxide (a-SiO<sub>x</sub>:H) as a buffer layer at the p/i interface of hydrogenated amorphous silicon germanium (a-SiGe:H) solar cells. This buffer layer was intended to effectively diminish the band discontinuity between the high-bandgap p-window layer and low-gap a-SiGe:H absorption layer, thereby enhancing the cell performance. The open-circuit voltage ( $V_{oc}$ ) increased by 3.7% as the [CO<sub>2</sub>]/[SiH<sub>4</sub>] gas ratio increased from 0 to 0.06. In addition, the short-circuit current density ( $J_{sc}$ ) gradually increased with the gas ratio. Using the optimized a-SiO<sub>x</sub>:H buffer layer, a high performance of 9.6% was recorded for narrow-gap a-SiGe:H thin film solar cells. a-SiGe:H solar cells with optimized a-SiO<sub>x</sub>:H buffer layers, used as middle subcells, are expected to enhance the total  $V_{oc}$  of triple-junction configuration solar cells.

© 2018 Elsevier B.V. All rights reserved.

## 1. Introduction

Thin-film silicon solar cells have been the subject of extensive research for many decades as solar energy-harvesting devices [1–4]. In spite of suffering from light-induced performance degradation upon light soaking, known as the Staebler–Wronski effect [5], their competitive advantages such as low production cost, large-scale manufacturing, flexibility, light weight, and especially their potential applicability to building-integrated photovoltaic systems have continued to foster further improvements [6–8]. In particular, the recent world-record achievements of triple-junction solar cells with initial performance of over 16% have paved the way for the persistent pursuit of high-performance and cost-effective solar cells [9,10].

The main advantage of the triple-junction configuration is the use of three absorption layers with different bandgaps for capturing the full range of solar spectra and thus increasing the cell performance. In the triple-junction configuration, generally, hydrogenated amorphous silicon germanium (a-SiGe:H) solar cells play an important role as the middle subcells, in combination with

hydrogenated amorphous silicon (a-Si:H) top cells and hydrogenated microcrystalline silicon ( $\mu$ c-Si:H) bottom cells. As middle subcells in this configuration, the a-SiGe:H active layers are supposed to gain an intermediate bandgap, generally in range of 1.4–1.6 eV [11], compared with the intrinsic 1.7–1.8 eV for the a-Si:H top cells and 1.1 eV for the  $\mu$ c-Si:H bottom cells. By varying the Ge content in the i-layer, the bandgap of the a-SiGe:H absorption layers can be changed over a large range of 1.1–1.8 eV [12]. Unfortunately, the narrow bandgap of a-SiGe:H layers normally results in band discontinuities [13–15], otherwise known as band-offset, compared with the high bandgap of p-type layers. This is mainly attributed to diminishing the open-circuit voltage ( $V_{oc}$ ) and fill factor (FF) [16,17]. A buffer layer at the p/i interface with an intermediate bandgap between those of the p-window layer and a-SiGe:H absorption layer has been proposed as a solution for the band discontinuity issue [2,16]. Buffer layers of a-Si:H have been effectively used to enhance the cell parameters of narrow-gap a-SiGe:H solar cells, especially  $V_{oc}$  and FF [2,10,18]. However, there is still scope to investigate tuneable-bandgap materials such as hydrogenated amorphous silicon carbide (a-SiC:H), a-SiGe:H, and a-SiO<sub>x</sub>:H to further enhance cell parameters. Owing to its two-terminal series electrical configuration, the  $V_{oc}$  of a triple-junction solar cell is approximately given by the sum of the  $V_{oc}$  values of the three subcells. Therefore, an enhancement in the  $V_{oc}$

\* Corresponding author.

\*\* Corresponding author.

E-mail addresses: [jwjh3516@skku.edu](mailto:jwjh3516@skku.edu) (J. Park), [junsin@skku.edu](mailto:junsin@skku.edu) (J. Yi).

of the a-SiGe:H middle subcells can improve the overall performance of the triple-junction configuration.

Consequently, this study aims to further enhance the cell parameters, especially  $V_{oc}$ , of narrow-gap a-SiGe:H solar cells. For this purpose, we examined a-SiO<sub>x</sub>:H materials with various bandgaps as buffer layers at the p/i interface of a-SiGe:H solar cells. The effect of these buffer layers on the cell parameters was discussed in comparison with the conventional a-Si:H buffer layer.

## 2. Experiment

We used a cluster multi-chamber plasma-enhanced chemical vapor deposition system for the fabrication of a-SiGe:H thin-film solar cells. All cells were fabricated in a p-i-n superstate configuration on commercial Fluorine doped Tin oxide (FTO)-coated glass substrates with the random roughness in range of 5–20 nm. The window layers were double p-type layers, including hydrogenated microcrystalline silicon oxide (p-μc-SiO<sub>x</sub>:H) and hydrogenated amorphous silicon oxide (p-a-SiO<sub>x</sub>:H) with optical bandgaps of 2.1 and 2.0 eV, respectively. The n-layers were hydrogenated microcrystalline silicon (n-μc-Si:H). The absorption layers or intrinsic layer (i-layers) were a-SiGe:H layers with a thickness of 300 nm and an optical bandgap of 1.58 eV. In order to smooth the p/i interface, the intrinsic a-SiO<sub>x</sub>:H buffer layers were inserted between the p- and i-layers.

Single a-SiO<sub>x</sub>:H layers of thickness 50 nm were deposited on eagle glass. The deposition parameters of these layers are exhibited in Table 1. The electrical properties, including the dark and photoconductivity, of the a-SiO<sub>x</sub>:H layers were measured with a paired aluminium planar electrode configuration using a semiconductor parameter analyser (EL420C). The thickness and absorption coefficient were inferred from fitting the ellipsometry spectra using the VASE J. A. Woollam system over a wavelength range of 240–1700 nm. Single a-SiGe solar cells were characterized under dark and illuminated conditions. A one-sun AM 1.5 solar tester with 100 mW/cm<sup>2</sup> light intensity was used for the illumination characterizations at 25 °C. The external quantum efficiency (EQE) model QEX7 was utilized.

## 3. Results and discussion

The main purpose of this work was to optimize the a-SiO<sub>x</sub>:H buffer layer at the p/i interface of narrow-gap a-SiGe:H solar cells to significantly limit the band discontinuity between high-bandgap p-type window layers and narrow-gap intrinsic a-SiGe:H layers, which is expected to enhance the cell parameters, resulting in improved cell performance. In the first step, we examined the optoelectronic properties of the single a-SiO<sub>x</sub>:H buffer layers with respect to modifying the [CO<sub>2</sub>]/[SiH<sub>4</sub>] gas flow ratios during preparation. Fig. 1 shows the optoelectronic properties of 50 nm single a-SiO<sub>x</sub>:H layers as a function of the [CO<sub>2</sub>]/[SiH<sub>4</sub>] gas flow ratios, including the transmittance (1a), optical bandgap inferred by Tauc's plot (1 b), dark conductivity ( $\sigma_d$ ), photo-conductivity ( $\sigma_p$ ), and photosensitive value (1c), which is defined as ratio of the photo-to-

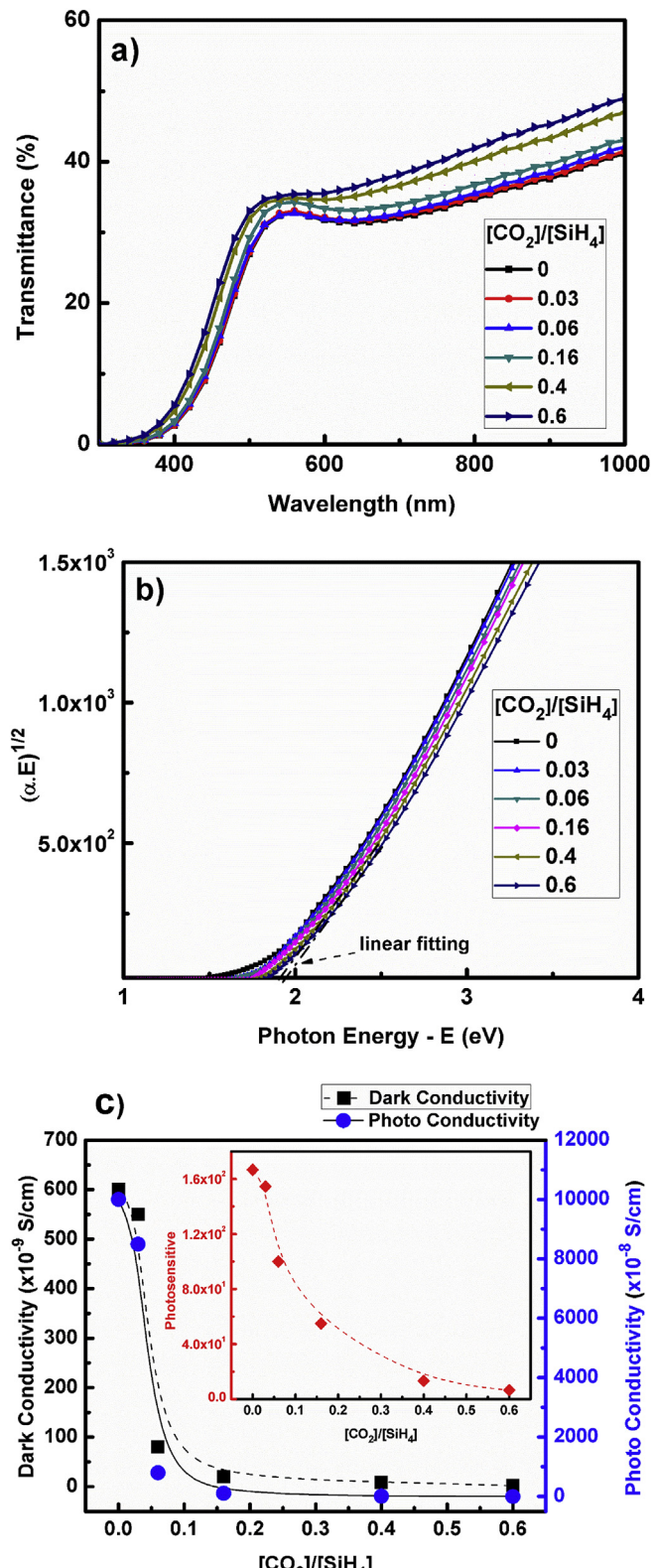


**Fig. 1.** a) Transmittance; b) Plot of  $(\alpha \cdot E)^{1/2}$  versus photon energy – E (the linear fitting, dash line, for determination of the Tauc optical bandgap); and c) Dark – and Photo – conductivity (the inset is the photosensitive which is determined by photo to dark conductivity ratio) of single a-SiO<sub>x</sub>:H layers.

**Table 1**

Deposition parameters of a-SiO<sub>x</sub>:H layers.

Parameters	Values
[H <sub>2</sub> ]/[SiH <sub>4</sub> ] flow ratio	5
[CO <sub>2</sub> ]/[SiH <sub>4</sub> ] flow ratio	0.0–0.6
Power density	42.55 mW/cm <sup>2</sup>
Working Pressure	300 mTorr
Deposition temperature	160 °C
Thickness	50 nm

dark-conductivities. The transmittance and optical bandgap of the films gradually increased with the gas ratios, whereas the electronic properties, such as  $\sigma_d$ , and  $\sigma_p$ , substantially decreased. It is well-known that the incorporation of oxygen elements into silicon thin-film materials can enhance the optical bandgap and therefore increase the transmittance [19–22]. In addition, this incorporation can cause high defect densities, reducing carrier transport, and as a result decreasing the conductivity [20,23]. The photosensitive value has been frequently used as one of the parameters to estimate the quality of a single silicon layer [24–26]. As seen in Fig. 1c, the photosensitive values gradually decreased with the gas ratios and especially decreased by one to two orders of magnitude at gas ratios greater than 0.06. The decrease in the photosensitive values suggested that the high oxygen concentration via the increased  $\text{CO}_2$  flow rate detrimentally affected the quality of the a-SiO<sub>x</sub>:H films, i.e., increased the defect density in the films.

In the second step, we fabricated single a-SiGe:H solar cells with various the  $[\text{CO}_2]/[\text{SiH}_4]$  gas flow ratios of the a-SiO<sub>x</sub>:H buffer at the p/i interface, as shown in Fig. 2. We examined the effect of the buffer layers on the cell parameters such as  $J_{sc}$ , FF, and  $V_{oc}$ . These parameters were extracted from the illuminated J-V curves, as shown in Fig. 3a. In addition, Fig. 3b summarizes the variation of these parameters with the gas ratios. First, as can be seen in Fig. 3b, the  $J_{sc}$  value regularly increased with the gas ratios. This increase is consistent with that in the transmittance and optical bandgap of the buffer layers as shown in Fig. 1. This means that the increase in  $J_{sc}$  could be due to the broadened optical bandgap of the buffers, resulting in reducing parasitic absorption and therefore enhanced transmittance, especially at short wavelengths, into the absorption a-SiGe:H layers. To demonstrate the enhanced short-wavelength absorption of the absorption layers, we examined the EQE measurements, as shown in Fig. 4. The results indicated the clear increase in the short wavelength of EQE with the gas ratios.

Second, the FF values in Fig. 3b decreased slightly from 0.66 to 0.64 as the  $[\text{CO}_2]/[\text{SiH}_4]$  gas flow ratio increased from 0.0 to 0.06, and dropped significantly when the ratio was higher than 0.16. The decrease in FF can be due to the reduced conductivity of the a-SiO<sub>x</sub>:H buffer layers with gas ratios, which can cause considerable increases in the series resistance ( $R_s$ ) value of the device. Based on the dark I–V characteristics [27], we calculated the  $R_s$  value of the a-SiGe:H cells, as shown in Fig. 5a. In addition, Fig. 5b summarizes

the  $R_s$  values of the cells as a function of the gas ratio. It can be seen that the  $R_s$  value gradually increases from  $8\ \Omega$  to  $14\ \Omega$  with the gas ratio. It is well-known that the FF value is proportional to the shunt resistance and inversely proportional to the series resistance of a cell device [28,29]. It can be inferred that the reduction in conductivity of the buffer layers with the gas ratio could result in an increase in  $R_s$  and therefore a reduction in the FF value.

Finally, the  $V_{oc}$  showed a low value of  $0.78\text{ V}$  with the conventional a-Si:H buffer layer, with  $[\text{CO}_2]/[\text{SiH}_4] = 0$ . The  $V_{oc}$  gradually increased to  $0.82\text{ V}$  at the ratio of 0.06 and abruptly decreased to  $0.79\text{ V}$  at the ratios higher than 0.06. We used the amorphous semiconductor analysis (ASA) simulation program to simulate the p/i interface with various a-SiO<sub>x</sub>:H buffer layers. The band diagram schematics of the cells are shown in Fig. 6. It can be observed that a significantly high potential barrier may be formed at the p/i interface of a cell without buffer layers. A conventional a-Si:H buffer layer can significantly reduce the band discontinuity with the i-layer, but considerably formed a band-offset with the p-layer. In addition, with high bandgap of the a-SiO<sub>x</sub>:H buffer layer at the gas ratio of 0.6, the considerably high band-offset was formed with the i-layer, but strongly reduced at the p-side layer. In all these cases, the hole carrier transport can be significantly hindered by high potential carriers, resulting in detrimental effects on  $V_{oc}$  and FF. Consequently, it is believed that the intermediate bandgap of the a-SiO<sub>x</sub>:H buffer layer at the gas ratio of 0.06 can balance the band-offset at both interfaces, as shown in Fig. 6, resulting in an enhancement in  $V_{oc}$ . D. Lundszien *et al* [14,16]. Investigated complete effects of a-Si:H buffer layers at the interfaces on narrow-gap a-SiGe:H solar cells. It showed clearly that a-Si:H buffer layers can improve significantly the cell parameters such as  $V_{oc}$  and FF, resulting in cell efficiency-enhancement. However, with a tendency to further widening the band gap of the window layers in order to enhance the light into the absorption layers [30–32], the a-Si:H buffer layers with the limited band gap seem to be a non-optimal choice for balancing the band discontinuity at the p/i interface. Consequently, tuneable-bandgap buffer layers such as a-SiC:H [18,33] or a-SiO<sub>x</sub>:H [20,23] layers can play a potential role in the band-offset challenge of narrow-gap a-SiGe:H solar cells.

In conclusion, a high conversion  $E_{ff}$  of 9.6% was found with the a-SiO<sub>x</sub>:H buffer with a  $[\text{CO}_2]/[\text{SiH}_4]$  gas flow ratio of 0.06. The cell parameters, including  $J_{sc}$  and particularly  $V_{oc}$ , were impressively

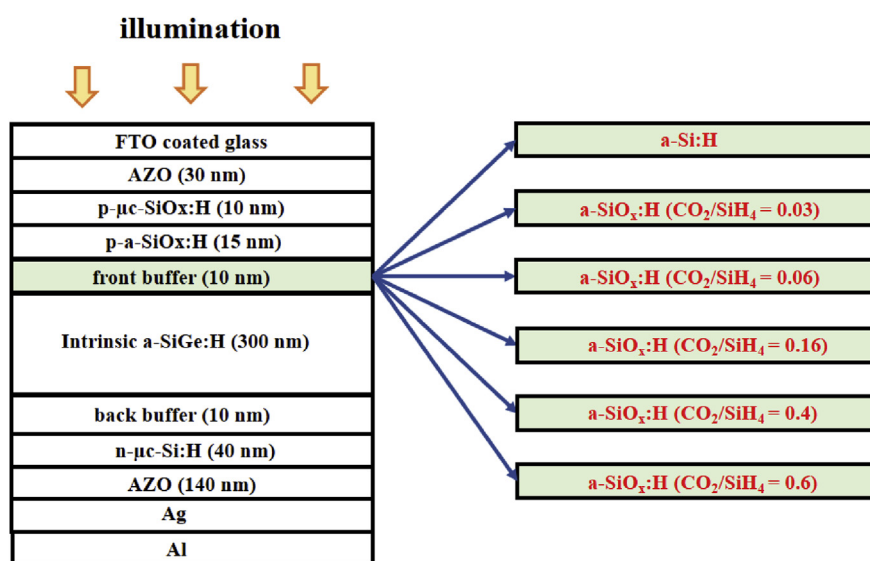
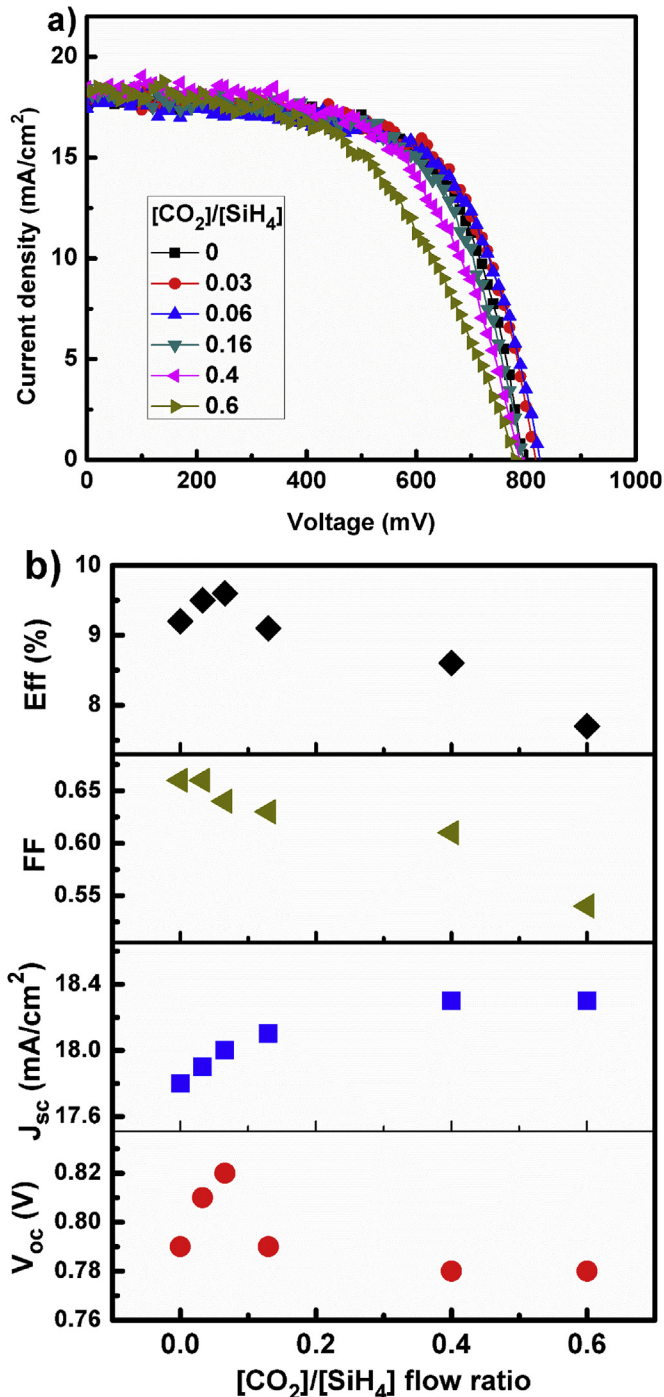
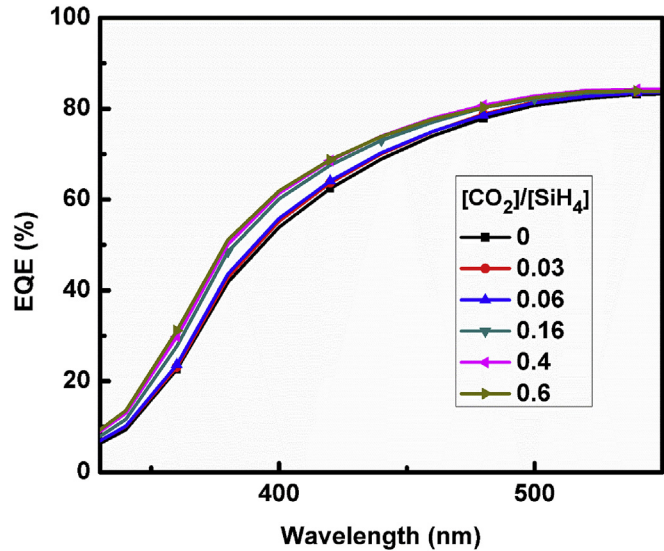


Fig. 2. Single a-SiGe:H cell structure with various the  $[\text{CO}_2]/[\text{SiH}_4]$  gas ratios of a-SiO<sub>x</sub>:H buffer layers.



**Fig. 3.** a) Illuminated J-V curve characteristics of a-SiGe:H solar cells; and b) variation of cell parameters such as  $V_{oc}$ ,  $J_{sc}$ , FF, and  $E_{eff}$  as a function of the gas ratios.

increased at this ratio, compared with those of the conventional a-Si:H buffer layer. The gradual increase in  $J_{sc}$  was attributed to the broadened optical bandgap of the a-SiO<sub>x</sub>:H buffer layer owing to changes in the  $[\text{CO}_2]/[\text{SiH}_4]$  gas ratios. The enhancement in  $V_{oc}$  could be due to the reduction in the band-offset at the p/i interface with the intermediate bandgap of a-SiO<sub>x</sub>:H at the gas ratio of 0.06, whereas the gradual decrease in FF may be due to the increase in the  $R_s$  value of the cell device.



**Fig. 4.** External quantum efficiencies of a-SiGe:H solar cells in short wavelength.

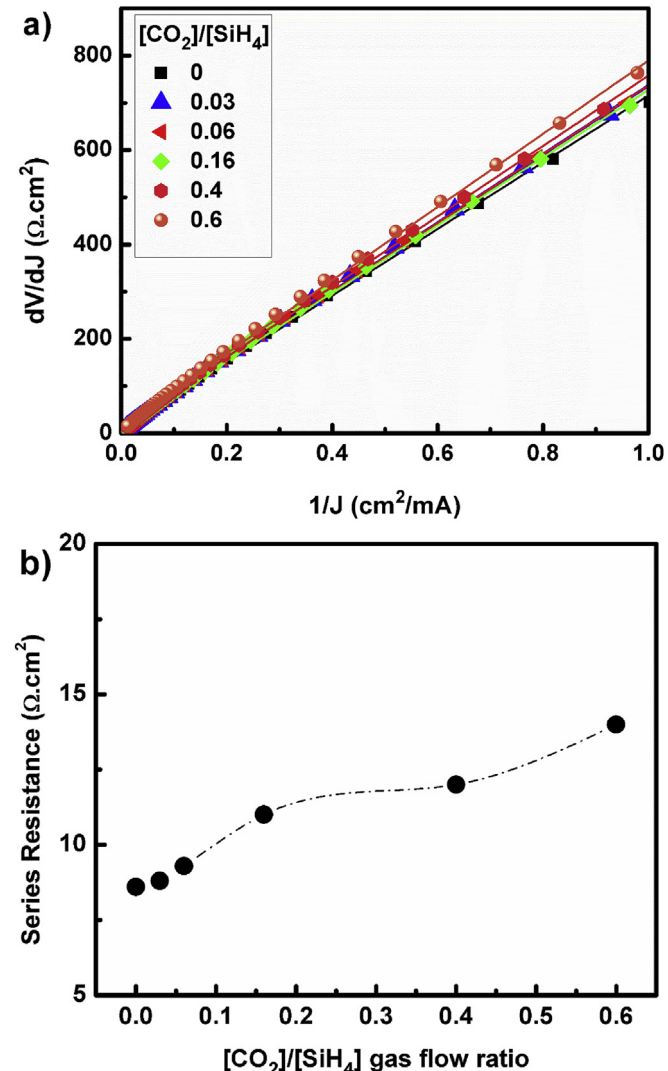


**Fig. 5.** a) Plot of  $dV/dJ$  vs  $1/J$  for a-SiGe:H solar cells from measured dark  $J(V)$  data. From the linear fitting, the intercept is series resistance ( $R_s$ ); and b) variation of  $R_s$  as a function of the gas ratios.

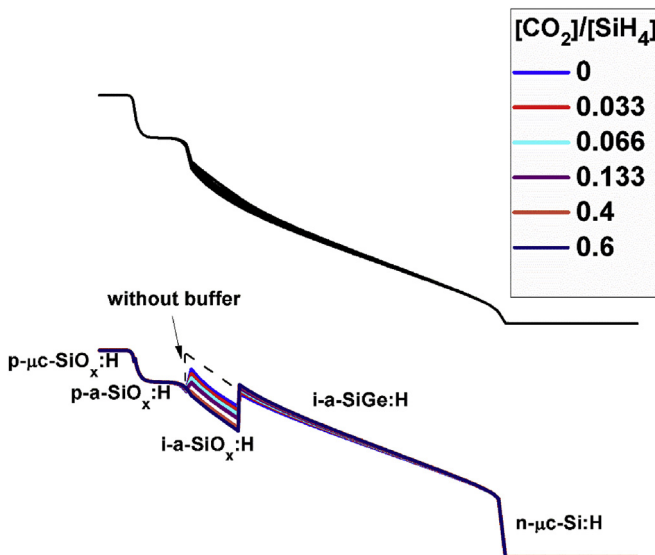


**Fig. 6.** The band diagrams of a-SiGe:H solar cells, extracted from the ASA simulation, with various the gas ratios of a-SiO<sub>x</sub>:H buffer layers.

#### 4. Conclusion

We optimized the a-SiO<sub>x</sub>:H buffer layers at the p/i interface for narrow-gap a-SiGe:H solar cells. The a-SiO<sub>x</sub>:H buffer layer with a [CO<sub>2</sub>]/[SiH<sub>4</sub>] gas ratio of 0.06 showed increases in V<sub>oc</sub> and J<sub>sc</sub> compared with the conventional a-Si:H buffer layer. A high cell efficiency of 9.6% was obtained with the a-SiO<sub>x</sub>:H buffer at this ratio. The a-SiO<sub>x</sub>:H buffer was credited with significantly diminishing the band-offset between the high-bandgap p-layer and narrow-gap intrinsic a-SiGe:H layer. With optimized a-SiO<sub>x</sub>:H buffer layers, the V<sub>oc</sub> values of a-SiGe:H solar cells are expected to be further improved. Therefore, the performance of the triple-junction configuration solar cells.

#### Acknowledgments

This work was supported by the New & Renewable Energy Core Technology Program of the Korea Institute of Energy Technology Evaluation and Planning (KETEP), granted financial resource from the Ministry of Trade, Industry & Energy, Republic of Kore (No. 20163010012230).

#### References

- [1] T. Matsui, M. Kondo, Advanced materials processing for high-efficiency thin-film silicon solar cells, *Sol. Energy Mater. Sol. Cell.* 119 (2013) 156–162.
- [2] D.P. Pham, S. Kim, J. Park, J. Cho, H. Kim, A.H.T. Le, J. Yi, Role of a-Si:H buffer layer at the p/i interface and band gap profiling of the absorption layer on enhancing cell parameters in hydrogenated amorphous silicon germanium solar cells, *Optik Int. J. Light Elect. Opt.* 136 (2017) 507–512.
- [3] D.P. Pham, S. Kim, J. Park, A.H.T. Le, J. Cho, J. Yi, Improvement in Carrier collection at the i/n interface of graded narrow-gap hydrogenated amorphous silicon germanium solar cells, *J. Alloys Compd.* 724 (2017) 400–405.
- [4] D.P. Pham, S. Kim, J. Park, A.T. Le, J. Cho, J. Jung, S.M. Iftiquar, J. Yi, Silicon germanium active layer with graded band gap and μc-Si:H buffer layer for high efficiency thin film solar cells, *Mater. Sci. Semicond. Process.* 56 (2016) 183–188.
- [5] D.L. Staebler, C.R. Wronski, Reversible conductivity changes in discharge-produced amorphous Si, *Appl. Phys. Lett.* 31 (4) (1977) 292–294.
- [6] J. Yang, A. Banerjee, S. Guha, Amorphous silicon based photovoltaics—from earth to the “final frontier”, *Sol. Energy Mater. Sol. Cell.* 78 (1–4) (2003) 597–612.
- [7] M. Konagai, Present status and future prospects of silicon thin-film solar cells, *Jpn. J. Appl. Phys.* 50 (2011), 030001.
- [8] P. Heinstein, C. Ballif, L.-E. Perret-Aebi, Building integrated photovoltaics (BIPV): review, potentials, barriers and Myths, *Greenpeace* 3 (2) (2013) 125–156.
- [9] B. Yan, G. Yue, L. Sivec, J. Yang, S. Guha, C.-S. Jiang, Innovative dual function nc-SiO<sub>x</sub>:H layer leading to a >16% efficient multi-junction thin-film silicon solar cell, *Appl. Phys. Lett.* 99 (11) (2011), 113512.
- [10] B. Liu, L. Bai, X. Zhang, C. Wei, Q. Huang, J. Sun, H. Ren, G. Hou, Y. Zhao, Fill factor improvement in PIN type hydrogenated amorphous silicon germanium thin film solar cells: omnipotent N type μc-SiO<sub>x</sub>:H layer, *Sol. Energy Mater. Sol. Cell.* 140 (2015) 450–456.
- [11] S. Guha, Thin film silicon solar cells grown near the edge of amorphous to microcrystalline transition, *Sol. Energy* 77 (6) (2004) 887–892.
- [12] P. Agarwal, H. Povolny, S. Han, X. Deng, Study of a-SiGe:H films and n-i-p devices used in high efficiency triple junction solar cells, *J. Non-Cryst. Solids* 299–302 (2002) 1213–1218.
- [13] J.-W. Chung, J.W. Park, Y.J. Lee, S.-W. Ahn, H.-M. Lee, O.O. Park, Graded layer modification for high efficiency hydrogenated amorphous silicon–germanium solar cells, *Jpn. J. Appl. Phys.* 51 (2012) 10NB16.
- [14] D. Lundszien, F. Finger, H. Wagner, A-Si:H buffer in a-SiGe:H solar cells, *Sol. Energy Mater. Sol. Cell.* 74 (2002) 365–372.
- [15] J. Cho, D.P. Pham, J. Jung, C. Shin, J. Park, S. Kim, A.H. Tuan Le, H. Park, S.M. Iftiquar, J. Yi, Improvement of hydrogenated amorphous silicon germanium thin film solar cells by different p-type contact layer, *Mater. Sci. Semicond. Process.* 41 (2016) 480–484.
- [16] D. Lundszien, F. Finger, H. Wagner, Band-gap profiling in amorphous silicon–germanium solar cells, *Appl. Phys. Lett.* 80 (9) (2002) 1655–1657.
- [17] R.J. Zambrano, F.A. Rubinelli, W.M. Arnoldbik, J.K. Rath, R.E.I. Schropp, Computer-aided band gap engineering and experimental verification of amorphous silicon–germanium solar cells, *Sol. Energy Mater. Sol. Cell.* 81 (1) (2004) 73–86.
- [18] B. Samanta, D. Das, A.K. Barua, Role of buffer layer at the p/i interface on the stabilized efficiency of a-Si solar cells, *Sol. Energy Mater. Sol. Cell.* 46 (1997) 233–237.
- [19] K. Yoon, C. Shin, Y.-J. Lee, Y. Kim, H. Park, S. Baek, J. Yi, The role of buffer layer between TCO and p-layer in improving series resistance and Carrier recombination of a-Si:H solar cells, *Mater. Res. Bull.* 47 (10) (2012) 3023–3026.
- [20] J. Park, V.A. Dao, C. Shin, H. Park, M. Kim, J. Jung, D. Kim, J. Yi, A buffer-layer/a-SiO<sub>x</sub>:H(p) window-layer optimization for thin film amorphous silicon based solar cells, *Thin Solid Films* 520 (2013) 331–336.
- [21] J. Park, C. Shin, S. Lee, S. Kim, J. Jung, N. Balaji, V.A. Dao, Y.-J. Lee, J. Yi, Effect of thermal annealing on the optical and electrical properties of boron doped a-SiO<sub>x</sub>:H for thin-film silicon solar cell applications, *Thin Solid Films* 587 (2015) 132–136.
- [22] C. Shin, S.M. Iftiquar, J. Park, S. Ahn, S. Kim, J. Jung, S. Bong, J. Yi, Radio frequency plasma deposited boron doped high conductivity p-type nano crystalline silicon oxide thin film for solar cell window layer, *Mater. Chem. Phys.* 159 (2015) 64–70.
- [23] J. Fang, Z. Chen, N. Wang, L. Bai, G. Hou, X. Chen, C. Wei, G. Wang, J. Sun, Y. Zhao, X. Zhang, Improvement in performance of hydrogenated amorphous silicon solar cells with hydrogenated intrinsic amorphous silicon oxide p/i buffer layers, *Sol. Energy Mater. Sol. Cell.* 128 (2014) 394–398.
- [24] L. Zhang, J. Zhang, X. Zhang, Y. Cao, Y. Zhao, Active roles of helium in the growth of hydrogenated microcrystalline silicon germanium thin films, *Thin Solid Films* 520 (18) (2012) 5940–5945.
- [25] R.J. Soukup, N.J. Ianno, S.A. Darveau, C.L. Exstrom, Thin films of a-SiGe:H with device quality properties prepared by a novel hollow cathode deposition technique, *Sol. Energy Mater. Sol. Cell.* 87 (1–4) (2005) 87–98.
- [26] B. Yan, L. Zhao, B. Zhao, J. Chen, G. Wang, H. Diao, Y. Mao, W. Wang, Hydrogenated amorphous silicon germanium alloy with enhanced photosensitivity prepared by plasma enhanced chemical vapor deposition at high temperature, *Vacuum* 89 (2013) 43–46.
- [27] S.S. Hegedus, Current-voltage analysis of a-Si and a-SiGe solar cells including voltage-dependent photocurrent collection, *Prog. Photovoltaics Res. Appl.* 5 (1997) 151–168.
- [28] M. Dadu, A. Kapoor, K.N. Tripathi, Effect of operating current dependent series resistance on the fill factor of a solar cell, *Sol. Energy Mater. Sol. Cell.* 71 (2002) 213–218.
- [29] D. Pyisch, A. Mette, S.W. Glunz, A review and comparison of different methods to determine the series resistance of solar cells, *Sol. Energy Mater. Sol. Cell.* 91 (18) (2007) 1698–1706.
- [30] H. Tan, P. Babal, M. Zeman, A.H.M. Smets, Wide bandgap p-type nanocrystalline silicon oxide as window layer for high performance thin-film silicon multi-junction solar cells, *Sol. Energy Mater. Sol. Cell.* 132 (2015) 597–605.
- [31] K. Yoon, Y. Kim, J. Park, C.H. Shin, S. Baek, J. Jang, S.M. Iftiquar, J. Yi, Preparation and characterization of p-type hydrogenated amorphous silicon oxide film and its application to solar cell, *J. Non-Cryst. Solids* 357 (2011) 2826–2832.
- [32] R. Biron, C. Pahud, F.J. Haug, C. Ballif, *J. Non-Cryst. Solids* 358 (2012) 1958–1961.
- [33] P. Chaudhuri, S. Ray, A.K. Batabyal, A.K. Barua, Performance dependence of a-Si/A-Si double junction solar cell on the quality of the a-Si:C: H buffer layer at p<sup>+</sup>-Si:C: H/i-a-Si:H interface, *Sol. Energy Mater. Sol. Cell.* 36 (1994) 45–50.